This is a “preproof” accepted article for Weed Science. This version may be subject to change in the production process, *and does not include access to supplementary material*.
DOI: 10.1017/wsc.2025.10056

Short title: *S. chamaejasme* in Degrad Grasslands

The Distribution Pattern of Chinese Stellaria (*Stellera chamaejasme*) in Degraded Grasslands of the Qilian Mountains

Weiwei Li[1](0009-0007-5721-3698), Ruiming Zhao[1]

[1]College of Agronomy, Gansu Agricultural University, Yingmen Village, Anning District, Lanzhou 730070, Gansu, China

Author for correspondence: Weiwei Li; Email: 1093961041@qq.com
Ruiming Zhao; Email: zhaorm1001@163.com

Abstracts: Chinese Stellaria (*Stellera chamaejasme* L.) is a indicator plant of degraded grasslands. With its robust vitality, once it emerges in grassland ecosystems, it undergoes extensive growth and rapid expansion, leading to grassland degradation as an inevitable consequence. The establishment and invasion of *S. chamaejasme* disrupts the ecological balance of grasslands in Qilian Mountains. This study was conducted in a grassland on the eastern slope of the Qilian Mountains, employing point pattern analysis to investigate the spatial distribution patterns of *S. chamaejasme* and the relationships among different age classes. The population was categorized into three growth stages: young, sub-adult, and mature plants. The results revealed that the spatial distribution of this population is primarily dominated by subadult plants, accounting for up to 75.48% of the total, with an overall transition trend from aggregated to random distribution. No significant spatial correlations were observed among different age groups (young, subadult plants, and mature plants), indicating that mature plants do not exert significant inhibitory effects on the growth of young individuals. In high-density areas, the population exhibited a radiating distribution outward from mature plants as the center, with high-density cores predominantly concentrated within 0-5 m. Significant density variations were observed between regions, with the highest total density estimated at approximately 9.57 plants/m² and the lowest at 2.68 plants/m². The invasion mechanism of *S. chamaejasme* is closely associated with the spatial independence of its age groups and a distribution pattern dominated by subadult plants. During the initial invasion phase, *S. chamaejasme* spreads predominantly around mature plants. After securing sufficient growing space (0–1 m), it further competes for territory through shifts in distribution patterns—transitioning from aggregated to random distribution. Additionally, significant differences in distribution density and expansion patterns across regions provide critical theoretical foundations for targeted ecological management strategies.

Keywords: *S. chamaejasme* L, Point pattern, Distribution pattern

https://doi.org/10.1017/wsc.2025.10056 Published online by Cambridge University Press

Introduction

Chinese Stellaria (*Stellera chamaejasme* L.) is a toxic perennial herbaceous plant commonly found in grasslands and meadows ranging from southern Russia to southwestern China and the western Himalayas (Zhang et al. 2010; Zhang et al. 2015). It is a traditional Chinese medicine with various medicinal properties, including antibacterial, insecticidal, dispersing, diuretic, analgesic, and expectorant effects (Selenge et al. 2023; Zhang et al. 2016). Beyond its medicinal value, *S. chamaejasme* has drawn significant attention for its destructive effects on grassland ecosystems (Cheng et al. 2004). The entire plant is toxic, with specific components such as stellaterpenoids A-M demonstrating notable cytotoxic activity (Pan et al. 2021). Livestock accidentally ingesting this plant exhibit severe poisoning symptoms including vomiting and convulsions, which can ultimately lead to death (Liu et al. 2018). Consequently, grazing animals selectively avoid consuming *S. chamaejasme*, intensifying grazing pressure on other forage species (You et al. 2018). This selective grazing behavior not only accelerates grassland degradation but also disrupts ecological balance. *Stellaria chamaejasme* has a strong reproductive capacity, with robust rhizomes and high soil nutrient conversion efficiency, which significantly suppresses the growth of surrounding plants, often becoming a dominant species on grasslands (Liu et al. 2022). Particularly in northern regions, *S. chamaejasme* has become a major invasive threat, infesting millions of hectares across multiple provinces - notably 1.4 million hectares in Qinghai and 546,700 hectares in Gansu. In Gansu Province alone, this invasion has caused annual losses of 137.5 million kilograms of forage and economic damages estimated at 15-20 million yuan (Wang et al. 2015). The plant's robust rhizomes and efficient nutrient conversion enable it to dominate degraded grasslands, with density increasing from 1.95 plants/m² in mildly degraded areas to 7.16 plants/m² in severely degraded ones (Liu et al. 2022). The proliferation of *S. chamaejasme* not only alters plant community structures (Gao et al. 2018) but also negatively impacts ecosystem services such as carbon sequestration, nutrient cycling, soil and water conservation, and water retention (Ren et al. 2013), leading to a gradual decline in the service value and capacity of grassland ecosystems (Cheng et al. 2014). As *S. chamaejasme* continues to expand, the dominant species shift from forage grass to *S. chamaejasme*, making it one of the most serious weed problems on Chinese grasslands (Guo et al. 2020).

https://doi.org/10.1017/wsc.2025.10056 Published online by Cambridge University Press

Current research on the dispersal mechanisms of *S. chamaejasme* has identified several key biological traits driving its invasion success. The species exhibits a robust root system capable of penetrating 60–100 cm (four-year-old individuals) into the soil, enabling efficient nutrient and water uptake even in adverse conditions (Li et al. 2019). Its drought-resistant lanceolate leaves (Lee et al. 2015), caespitose stems with terminal inflorescences facilitating pollination (Huang et al. 2014), and prolific seed production (200 seeds per mature plant) further enhance its reproductive efficiency (Zhao and Wang 2011). The hard-shelled nutlet fruit also ensures long-term seed viability despite livestock trampling (Wu et al. 2014). Notably, the plant's toxicity and allelopathic effects suppress herbivory and inhibit neighboring plant growth (Cheng et al. 2017; Wang et al. 2022), while its secondary metabolites alter soil properties and microbial communities, creating self-favorable microhabitats (An et al. 2016; Zhang et al. 2021). The aqueous extract of *S. chamaejasme* contains toxic flavonoids that effectively deter herbivory by grazing animals, while its allelopathic compounds inhibit the normal growth of neighboring plants in grasslands (Liu et al. 2022; Li et al. 2022; Yan et al. 2014). This plant species strategically modifies its rhizosphere environment by altering soil physicochemical properties and reducing nutrient cycling in the root zone, thereby creating favorable conditions for its own proliferation (Zhu et al. 2020; Zhang et al. 2021). Furthermore, *S. chamaejasme* enhances its competitive advantage by increasing the abundance of soil-borne pathogenic fungi that suppress surrounding vegetation, while simultaneously being protected from these pathogens through its inherent flavonoid constituents, such as neochamaejasmin B, chamechromone, and isochamaejasmin (Yan et al. 2015). The plant's ecological dominance is further reinforced by its capacity to increase the diversity and richness of soil microbial communities, ultimately establishing a self-sustaining microenvironment that promotes its vigorous growth (Bao et al. 2020; Cui et al. 2020).

Population structure also plays a critical role on the dispersal mechanisms of *S. chamaejasme*: seedlings exhibit a maternal distribution pattern near parent plants (Gao et al. 2014), and spatial distributions shift from clumped to random or uniform with increasing altitude or grassland degradation, reflecting adaptive niche expansion (Gao et al. 2011). However, some gaps persist in understanding the ecological mechanisms underlying these patterns. Some studies have focused on small-scale analyses (0–2 m) of population structure and in-

https://doi.org/10.1017/wsc.2025.10056 Published online by Cambridge University Press

traspecific interactions (Gao et al. 2019; Zhao et al. 2010), justified by the species' limited seed dispersal radius (<0.5 m) and "near-mother" distribution (Bai 2024). Yet, the aforementioned studies are limited to a single region and overlook the differences in population spatial patterns across different regions (for example, the variations in spatial patterns and spatial relationships may be shaped by different soil heterogeneity and climate conditions in different grasslands). Furthermore, the ecological functions of age-class interactions from spatial patterns (competition or facilitation between seedlings and mature plants) remain poorly resolved. For instance, while hypotheses suggest competitive suppression of seedlings by mature plants (Gao et al. 2011), empirical evidence for such dynamics is lacking.

To address these gaps, this study integrates point pattern analysis to investigate how small-scale spatial patterns of *S. chamaejasme* in different regions (In five grasslands from the meadow regions of the Qilian Mountains). Specifically, we hypothesize: (1) *S. chamaejasme* exhibits distinct spatial distribution patterns across age classes (whole population, young, subadult, mature) in degraded grasslands, and the spatial distribution of *S. chamaejasme* is primarily driven by subadult plants. By analyzing spatial point patterns and correlations among age classes, this work aims to elucidate the mechanisms behind its dominance in degraded grasslands, providing critical insights for targeted ecological management and restoration strategies. (2) There are facilitation spatial effects of mature plants on seedling establishment, enabling rapid grassland invasion through age-class independence and localized maternal facilitation. By synthesizing density mapping with correlations among age classes, this work aims to elucidate its expansion dynamics in degraded ecosystems, establishing a predictive framework for modeling invasion trajectories and guiding evidence-based intervention strategies in grassland restoration.

Methods

Study area

The experiment selected representative natural alpine grasslands on the eastern side of the Qilian Mountains (Figure 1), located in the subalpine and alpine regions of the Qilian Mountain range, which belongs to the cold and humid climate type. This area exhibits distinct

https://doi.org/10.1017/wsc.2025.10056 Published online by Cambridge University Press

continental climate characteristics, with long, cold, and dry winters, and short, cool, and moist summers (Liu et al. 2024). Precipitation is concentrated mainly from May to September, and as altitude increases, temperatures gradually decrease while rainfall increases, creating a gradient of temperature and precipitation from the foothills to the deeper mountain areas (Tang et al. 2020). Based on the natural distribution patterns and population densities of *S. chamaejasme*, five sampling areas were established, namely Tian zhu Tibetan Autonomous County (TZ), Huang cheng Grassland (HC), Xi shui Nature Reserve Station (XS), Shan dan Military Horse Farm in Zhangye City (JM), and Kang le Grassland (KL) (Table 1).

Data collection

Five representative grassland plots dominated by *S. chamaejasme* were systematically selected along an 837-km transect on the eastern Qilian Mountains. Within each *S. chamaejasme* habitat, standardized 15 m × 15 m sampling quadrats were established. A Cartesian coordinate system was implemented in each quadrat, with the southeastern corner designated as the origin for spatial referencing. This geospatial framework enabled precise mapping of all *S. chamaejasme* individuals through Cartesian coordinates. Spatial distribution patterns and inter-age class correlations within *S. chamaejasme* populations were quantitatively analyzed using coordinate-derived positional data. Population density distributions were calculated per unit area, with particular emphasis on comparative analysis of density variations across different developmental stages. These spatial metrics were subsequently employed to elucidate invasion mechanisms underlying *S. chamaejasme* colonization in degraded grassland ecosystems.

Experimental methods

According to the classification criteria proposed by Guo et al. (2020) (Table 2), the *S. chamaejasme* population was divided into two growth stages: young plants (I-II) and mature plants (III-X). Here, we further subdivided the mature plant category into subadult plants (III-IV) and mature plants (V-X).

To assess the spatial patterns among the different age classes of young plants, subadult plants, and mature plants, we utilized the univariate pair correlation function g(r) (Stoyan and

https://doi.org/10.1017/wsc.2025.10056 Published online by Cambridge University Press

Stoyan 1994; Wiegand and Moloney 2004) under a homogeneous Poisson null model. We adopted the homogeneous Poisson process, which assumes Complete Spatial Randomness (CSR), for exploratory analysis across different age classes, demonstrating that the CSR distribution holds at approximately 0–3 m, indicating a spatial pattern consistent with randomness.

$$g_{(r)} = \frac{1}{\lambda^2} \cdot \frac{1}{2\pi r} \cdot \frac{d}{dr}\left(\frac{k(r)}{r}\right)$$

λ: The density of the point pattern (the number of points per unit area).

r: Spatial scale, referring to the radius of distance considered between points. It can be any value greater than 0.

dk(r)/dr: The derivative of the K function with respect to the radius *r*. It represents the rate of change in the deviation of the point pattern from a completely random distribution at the distance scale *r*.

2πr: This factor is used to convert the derivative of the K function into a probability density function, ensuring that *g*(*r*) has the correct dimensionality in space, thus making it a probability density function.

We examined the correlation between different age classes by employing the bivariate $g_{12}(r)$ function with the application of a random label null model (Aakala et al. 2007; Marzano et al. 2012). For the analysis, we pooled the location data of the various age classes.

$$g_{12}(r) = \frac{1}{\lambda_1 \lambda_2} \cdot \frac{1}{2\pi r} \cdot \frac{d}{dr}\left(\frac{k_{12}(r)}{r}\right)$$

λ_1 $\lambda_{2:}$ The densities of the point patterns marked as 1 and 2, respectively (the number of points per unit area). These densities are used to normalize the values of *g*12(*r*) so that it is not affected by the density of the point patterns.

$K_{12}(r)$: The cross-type *K*-function, which describes the number of point pairs between points marked as 1 and points marked as 2 within a distance *r*.

$dk_{12}(r)/dr$: The derivative of $K_{12}(r)$ with respect to the radius *r*, reflecting the rate of change in deviation from complete spatial randomness at the distance scale *r*

https://doi.org/10.1017/wsc.2025.10056 Published online by Cambridge University Press

For all the analyses, significant departure from the null models was evaluated based on 95% simulation envelopes, which were calculated from the 5th-lowest and 5th-highest values of 99 Monte Carlo simulations. A distribution is classified as clumped, random or regular for univariate analysis, when the value is located above, inside or below the 95% confidence intervals, respectively. Similarly, for bivariate analysis, two populations are significantly positively correlated (attraction), spatially independent or significantly negatively correlated (repulsion), when the value is located above, inside or under the 95% confidence intervals, respectively.

All univariate and bivariate point pattern analyses was conducted using the 'spatstat' package in R. Additionally, contour and density distribution maps were generated by integrating 'ggplot2', 'ggmap' and 'sf' packages with R.

Results and Discussion

Age structure

The specific distribution quantities and locations of *S. chamaejasme* across different age structures is depicted in Figure 2. Within the quadrats, the highest number of *S. chamaejasme* individuals is found in HC with 2153 plants (b, g), while the lowest is in TZ with only 604 plants (a, f). Overall, the *S. chamaejasme* population is predominantly composed of subadult plants, with proportions of 68.21%, 75.48%, 70.96%, 62.27%, and 71.60% (a-e). In terms of mature plants, the highest number is observed in KL with 229 plants (e, j), followed by TZ with 122 plants (a, f), and the lowest in JM with only 12 plants (d, i). Notably, in TZ, HC, and KL, the distribution of *S. chamaejasme* is markedly centered around mature plants (f, g, j). This pattern suggests that in these areas, the *S. chamaejasme* population is dominated by adult individuals, which may have significant implications for the stability and ecological functions of the population.

Spatial pattern

The g(r) univariate function reveals the distribution pattern of *S. chamaejasme* individuals at specific scales (Figure 3). In the TZ sampling site, the distribution pattern of *S. chamaejasme* total plants is similar to that of subadult plants, with initial aggregation within

https://doi.org/10.1017/wsc.2025.10056 Published online by Cambridge University Press

0-1 m followed by random distribution beyond 1 meter (a, c). Young plants exhibit a random distribution (a), while mature plants show an aggregated distribution (d). In the HC sampling site, aside from mature plants which follow a pattern of initial aggregation within 0-1 m followed by random distribution beyond 1 meter (h), the rest of the plants are aggregated (e-g). In the XS sampling site, except for young plants which are aggregated (j), the rest exhibit a pattern of initial aggregation followed by randomness, with the aggregation scale for total and subadult plants being 0-3 m (I, k), and for mature plants, it is 0-1 meter (l). In the JM sampling site, the distribution pattern for total and subadult plants is initial aggregation followed by randomness, with the random distribution primarily occurring beyond 2 m (m, o), while young and mature plants are generally randomly distributed (n, p). In the KL sampling site, young and mature plants are generally randomly distributed (r, t), whereas total and subadult plants are predominantly aggregated (q, s).

At this scale, the overall distribution pattern of *S. chamaejasme* (a, e, i, m, q) transitions from clustering to random distribution, with the exception of HC and KL, which remain clustered. The young plants are predominantly clustered, except for JM and KL, which are randomly distributed. The distribution pattern of subadult plants closely mirrors the overall pattern, likely due to the fact that subadult plants typically constitute the majority of the *S. chamaejasme* population. Mature plants are primarily randomly distributed, with the exception of TZ, which shows a clustering distribution, this may be caused by differences in the number of individuals in the maturity plant.

Spatial correlation

By employing the bivariate function $g_{12}(r)$, we are able to assess the spatial correlation between different age groups of *S. chamaejasme* at a specific scale (Figure4). The analysis reveals that there is no significant correlation between young plants and subadult plants (Y-S), young plants and mature plants (Y-M), or subadult plants and mature plants (S-M) at the 1-3m scale, with no apparent spatial positive or negative correlations observed. This finding indicates that different age groups of *S. chamaejasme* are spatially independent, meaning the distribution of one age group does not influence the distribution of the others. Such independence suggests limited likelihood of intraspecific competition and mutualistic symbiosis,

https://doi.org/10.1017/wsc.2025.10056 Published online by Cambridge University Press

implying that mature plants are unlikely to significantly inhibit or affect the normal growth of young plants. This spatial independence is beneficial for the adaptability, stability of the population, and the overall health of the ecosystem.

Density

In each group, the first column shows the density of mature plants, the second column shows the density of S-M plants, and the third column represents the total plants density (Figure 5). Upon comparative analysis, a significant similarity is observed between the total plant density map and the S-M plant density map. This indicates that the distribution characteristics of the *S. chamaejasme* population are primarily influenced by the number of S-M plants. Outside the TZ region, the total plant density is notably higher than the S-M plant density, a difference likely attributed to the inclusion of young plants. However, in the TZ region, where the number of young plants is relatively low, this difference is less pronounced. Further analysis reveals that the high-density areas in the S-M plant density map often radiate outward from the high-density areas in the mature plant density map. This pattern aligns with the clumped distribution feature of *S. chamaejasme*, suggesting that new plants tend to establish near the parent plants.

Specifically, the high-density distribution centers in the TZ and XS regions are similar, both within the range of 10-15 m (b, h); the high-density distribution centers in the HC and JM regions are similar, both within the range of 0-5 m (e, k); while the high-density distribution center range in the KL region is larger, spanning 0-15 m (n). From the total plant distribution density map, it can be observed that the distribution density value in the HC region is the highest (f), while the distribution density value in the TZ region is the lowest (c). Meanwhile, the highest distribution density values in the XS, JM, and KL regions show similarity (i, l, o). This demonstrates that there are evident differences and characteristics in the distribution density of *S. chamaejasme* across different regions, which may be caused by factors such as environmental conditions, soil fertility, and light exposure.

https://doi.org/10.1017/wsc.2025.10056 Published online by Cambridge University Press

Discussion

S. chamaejasme is recognized as an indicator plant for degraded grasslands due to its extensive growth and rapid invasion characteristics (Li et al. 2019). Since *S. chamaejasme* has caused serious damage to the ecological balance of grasslands, it is of great significance to investigate the reasons for its rapid invasion. This phenomenon is not only related to the biological characteristics (He et al. 2019), allelopathic effects (Song et al. 2023), and soil regulation capabilities of *S. chamaejasme* **(**Zhu et al. 2020), but also closely linked to its spatial distribution patterns (Gao et al. 2019). This study indicates that the spatial distribution of *S. chamaejasme* populations varies across different regions, yet there are also distinct commonalities. The overall distribution pattern and the distribution pattern of juvenile plants are quite different from each other. However, the overall distribution pattern of *S. chamaejasme* is highly similar to that of subadult plants, which can also be interpreted as the distribution pattern of the entire *S. chamaejasme* community being dominated by subadult plants.

The distribution pattern of *S. chamaejasme* hereafter referred to as exhibits an overall transition from aggregated to random distribution, consistent with findings reported by Ren et al. (2015). Under highly heterogeneous environmental conditions, plant populations typically display aggregated distribution patterns, potentially due to individual clustering in resource-rich habitat patches or facilitation through intraspecific positive interactions (Daleo et al. 2023). Conversely, random distribution tends to emerge in the absence of significant intraspecific interactions (O'Dwyer et al. 2018). This distributional transition in *S. chamaejasme* facilitates its growth and expansion. During early grassland succession, *S. chamaejasme* lacks competitive advantages due to smaller individual size, limited resource acquisition capacity, and reduced resistance to interspecific competition and sandstorm disturbances, necessitating aggregated distribution to enhance risk resilience (Ren et al. 2015). As it becomes a dominant species, the distribution pattern naturally shifts toward non-aggregated forms, enabling more uniform resource utilization and reducing over-reliance on singular resources, thereby enhancing population stability and adaptability (Wiegand et al. 2023).Previous studies indicate that the transition from aggregated to non-aggregated distribution with increasing invasion intensity reflects a shift in intraspecific relationships from

https://doi.org/10.1017/wsc.2025.10056 Published online by Cambridge University Press

facilitation to competition (Ren et al. 2013). This behavioral shift promotes patch expansion, coalescence, and numerical proliferation of *S. chamaejasme* populations (Gao et al. 2019). Notably, in HC and KL regions, *S. chamaejasme* maintains persistent aggregated distribution across scales, suggesting exceptional environmental adaptation. The higher population density and abundance in these areas imply superior habitat suitability, where soil resources sustain greater *S. chamaejasme* density per unit area, potentially explaining this regional divergence.

Furthermore, the overall distribution pattern of *S. chamaejasme* closely aligns with that of subadult individuals, indicating their dominance in shaping population spatial structure. Quantitative surveys revealed subadult plants constitute over 60% of *S. chamaejasme* populations, reflecting both demographic structure and adaptive strategies across habitats. The aggregated distribution of subadults likely stems from limited seed dispersal capacity, promoting germination near maternal plants, and potential survival benefits from intraspecific facilitation within clusters (Luo et al. 2021). Consequently, the numerical dominance and spatial characteristics of subadult plants significantly influence the overall distribution pattern of *S. chamaejasme* populations.

The most notable finding of this study is the lack of significant spatial correlations among different age classes of *S. chamaejasme*. This discovery effectively explains the species' rapid invasion of grasslands, as the absence of resource competition among individuals reduces major growth constraints. Spatial independence between age classes enables populations to utilize limited resources more efficiently, alleviating growth suppression caused by resource competition and thereby enhancing overall survival probability and reproductive success (Zhang et al. 2020). Second, such spatial independence may create diverse habitats and resource niches for other species, increasing ecosystem species richness and niche breadth, which strengthens ecosystem stability and functionality (Wiegand et al. 2021). This aligns with Cheng et al. (2014), who found that *S. chamaejasme* can protect neighboring plants from overgrazing by livestock. Additionally, *S. chamaejasme* is rarely consumed by herbivores due to its chemical defenses or unpalatability, prompting herbivores to shift their foraging to other plant species (You et al. 2018). This selective foraging behavior compresses the habitat space and reduces resource utilization efficiency of other plants, while *S. chamaejasme* exploits limited resources more effectively. Studies demonstrate that plant life

https://doi.org/10.1017/wsc.2025.10056 Published online by Cambridge University Press

stages in resource-abundant environments may exhibit reduced interdependence (Wang et al. 2023), as ample resources diminish interactions between individuals, allowing age classes to grow relatively independently (Akram et al. 2022). This mechanism directly facilitates the spatial independence and expansion of *S. chamaejasme*.

This study further reveals that *S. chamaejasme* exhibits a distinct distribution pattern centered around mature plants. This phenomenon may arise because larger clumps provide shelter for smaller individuals (Gao et al. 2011) or because microhabitats created by mature clumps (accumulated plant litter) supply essential nutrients for the growth of younger clusters (Durán-Rangel et al. 2012). Such a pattern not only enhances population stability but also ensures the growth and reproduction of juvenile plants, significantly facilitating *S. chamaejasme*'s grassland invasion. High-density zones of *S. chamaejasme* populations typically radiate outward from areas dominated by mature plants, indicating a preference for establishment near adult individuals. This distribution pattern reduces interspecific competition while securing favorable conditions for juvenile growth, thereby supporting the species' proliferation and invasion success. Importantly, these findings offer critical insights for management strategies. Controlling the density of mature plants may effectively curb *S. chamaejasme* expansion, as mature individuals serve as focal points for seedling establishment and growth.

This study elucidates the invasion mechanisms of *S. chamaejasme* and provides insights for its control and grassland restoration. During the initial invasion phase, *S. chamaejasme* spreads predominantly around mature plants (Figure 5), which facilitate the establishment of juveniles and subadults by offering shelter and improving microhabitat conditions. After securing initial growth space (0–1 m), juveniles and subadults compete for resources through aggregated distribution. As their competitive dominance increases (1–3 m), spatial patterns gradually transition from aggregated to random distribution, accelerating grassland invasion. However, under favorable soil conditions, *S. chamaejasme* maintains aggregated distribution to maintain high density per unit area, reinforcing its spatial dominance (Figure 3). Simultaneously, the lack of significant correlations among different age classes minimizes intraspecific resource competition, enabling efficient resource utilization and enhancing population survival and reproductive success (Figure 4).

https://doi.org/10.1017/wsc.2025.10056 Published online by Cambridge University Press

The overall distribution pattern of *S. chamaejasme* is primarily driven by subadult plants. Therefore, control and restoration efforts should prioritize monitoring the growth dynamics of subadult populations. However, due to weak inter-age correlations, strategies targeting a single age class may yield limited effectiveness. Given that mature plants dominate invasion centers, their control remains essential. An integrated strategy managing both mature and subadult plants is critical. During early invasion stages, focus should be on mature plant control. Mechanical mowing sustained for 3 years can be employed, concurrently combined with autumn mowing and reseeding to optimize grassland restoration (Li et al. 2021). For reseeding, Mongolian wheatgrass (*Elymus dahuricus* Turcz.) and crested wheatgrass [*Agropyron cristatum* (L.) Gaertn.] are recommended, as studies indicate their tolerance to the allelopathic effects of *S. chamaejasme* (Liu et al. 2019). However, mechanical mowing may cause ecosystem damage. Although reseeding mitigates this issue, it becomes logistically impractical during advanced invasion stages due to the overwhelming workload. Therefore, control efforts during later phases should shift to subadult plants. Given their large numbers, a combined chemical-physical approach such as mowing followed by targeted herbicide application is suggested. The herbicide formulation "675mL·hm-2 Langdujing + 112.5mL·hm-2 organosilicon adjuvant" is recommended, as it effectively controls *S. chamaejasme* while reducing the damage to forage grasses caused by using "Langdujing" alone (Bao et al. 2015). This approach is expected to prove effective. Consequently, future research should prioritize spatial distribution analysis to identify factors driving the distribution heterogeneity of S. *chamaejasme* across grasslands. Comparative studies of regional environmental variables could clarify its habitat preferences, enabling targeted control through population suppression and soil amendments altering soil fertility to create unfavorable growth conditions. These methods would not only curb invasion but also advance theoretical frameworks for grassland ecosystem restoration.

Funding

No funding was received for this work.

Declaration of Competing Interest

The authors declare that they have no known competing financial interests or personal relationships that could have appeared to influence the work reported in this paper.

Data Availability

Data will be made available on request.

References.

Aakala T, Kuuluvainen T, De Grandpré L, Gauthier S (2007) Trees dying standing in the northeastern boreal old-growth forests of Quebec: spatial patterns, rates, and temporal variation [J]. Can J Forest Res 37:50–61

Akram M A, Zhang Y, Wang X, Shrestha N, Malik K, Khan I, Ma W, Sun Y, Li F, Ran J, Deng J (2022) Phylogenetic independence in the variations in leaf functional traits among different plant life forms in an arid environment [J]. J Plant Physiol 272:153671

An D Y, Han L, Wu J Y, Chen J, Yuan Y Y, Liu Y, Wang Q H (2016) Effects of S*tellera chamaejasme* on soil properties of grassland in farming-pastoral zone in north China [J]. Acta Agrestia Sinica 24:559

Bai H L (2024) Analysis of Plant Community Characteristics and Population Patterns of *Stellera chamaejasme* in Degraded Meadow Steppes [D]. Inner Mongolia Normal University. https://doi.org/10.27230/d.cnki.gnmsu.2024.001079

Bao G S, Song M L, Wang Y Q, Yin Y L, Wang H S (2020) Effects of grazing exclosure and herbicide on soil physical-chemical properties and microbial biomass of *Stellera chamaejasme* patches in degraded grassland [J]. Acta Prataculturae Sinica 29:63

Bao G S, Wang H S, Zeng H (2015) Effects of adding organosilicon adjuvants to Langdujing on enhancing control effect and plant diversity of grassland communities. Pratacultural Science 32:263-268 (in Chinese)

Cheng W, Sun G, Du L F, Wu Y, Zheng Q Y, Zhang H X, Liu L, Wu N (2014) Unpalatable weed *Stellera chamaejasme* L. provides biotic refuge for neighboring species and conserves plant diversity in overgrazing alpine meadows on the Tibetan Plateau in China [J] Journal of

Mountain Science 11:746-754 (in Chinese)

Cheng W, Zhong B, Xu L Y, Du L F, Song K (2017) Allelopathic effects of root aqueous extract of different age of *Stellera chamaejasme* on four common plants in alpine meadow of Tibet Plateau [J] Ecological Science 36:1-11

Cheng Z, Sheng Y P, Cui Q Y, Xue B H (2004) Study on vegetation community's structure of degraded grassland of noxious and miscellaneous grass type. Journal of Desert Research 24:507-511 (in Chinese)

Cui X, Pan Y, Wang Y N, Zheng X N, Gao Y (2020) Effects of *Stellera chamaejasme* on small scale community composition and soil physical and chemical properties in degraded grassland. Chinese Journal of Ecology 39:2581

Daleo P, Alberti J, Chaneton E J, Iribarne O, Tognetti P M, Bakker J D, Borer E T, Bruschetti M, MacDougall A S, Pascual J, Sankaran M, Seabloom E W, Wang S, Bagchi S, Brudvig L A, Catford J A, Dickman C R, Dickson T L, Donohue I, Eisenhauer N, Gruner D S, Haider S, Jentsch A, Knops J M H, Lekberg Y, McCulley R L, Moore J L, Mortensen B, Ohlert T, Pärtel M, Peri P L, Power S A, Risch A C, Rocca C, Smith N G, Stevens C, Tamme R, Veen G F C, Wilfahrt P A, Hautier Y (2023) Environmental heterogeneity modulates the effect of plant diversity on the spatial variability of grassland biomass. Nat Commun. 14:1809

Durán-Rangel C, Gärtner S, Hernández L, Reif A (2012) Do microhabitats in forest gaps influence tree regeneration? A study in the montane forests of Venezuelan Guayana. Ecotropica 2:93-104

Gao F Y, Li K M, Zhao C Z, Ren H, Nie X Y, Jia D Y, Li L F, Li Q F (2019) The expansion process of a *Stellera chamaejasme* population in a degraded alpine meadow of Northwest China. Environ. Sci Pollut Res 26:20469-20474

Gao F Y, Shi F X, Chen H M, Zhang X H, Yu X Y, Cui Q, Zhao C Z (2018) Rapid expansion of Melica przewalskyi causes soil moisture deficit and vegetation degradation in subalpine meadows. CLEAN–Soil, Air, Water 46:1-11

Gao F Y, Zhao C Z, Shi F X, Sheng Y P, Ren H, He G B (2011) Spatial pattern of *Stellera chamaejasme* population in degraded alpine grassland in northern slope of Qilian Mountains, China. Chinese Journal of Ecology 30:1312-1316

Gao F Y, Zhao C Z, Zhuo M L C (2014) Spatial distribution pattern and spatial association of

https://doi.org/10.1017/wsc.2025.10056 Published online by Cambridge University Press

Stellera chamaejasme populations at different altitude gradients in alpine degraded grasslands. Acta Ecologica Sinica 34:605-612 (in Chinese)

Guo L Z, Zhao H, Lu J Y, Wang K L, Liu K S, Wang K, Huang D (2020) Population structure and quantitative dynamics of *Stellera chamaejasme* in degraded typical steppe. The Journal of Applied Ecology 31:2977-2984

He W, Detheridge A, Liu Y, Wang L, Wei H, Griffith G, Scullion J, Wei Y (2019) Variation in Soil Fungal Composition Associated with the Invasion of *Stellera chamaejasme* L. in Qinghai-Tibet Plateau Grassland. Microorganisms 12:587

Huang L C, Jin L, Li J, Zhang X Q, Yang Y, Wang X J (2014) Floral morphology and its relationship with pollination systems in Papilionoideae. Acta Ecol Sin 34:5360-5368

Lee S B, Suh M C (2015) Advances in the understanding of cuticular waxes in Arabidopsis thaliana and crop species. Plant Cell Rep 34:557-572

Li S F, Song M L, Wang Y Q, Wang H S, Yin Y L (2021) Effect of simulated autumn grazing on the community of degraded grassland after control of *Stellera chamaejasme*. Grassland and Turf 41:23-29

Li X H, Xiang X, Tang X P, Jiang H C, Duan G, Chang H (2019) Progress on *Stellera chamaejasme.* Progress in Veterinary Medicine 40:96-99

Li Y F, Chu X H, Li J Y, Ma Z Y, Niu J M, Dan G L (2022) Allelopathic Effects of Euphorbia jolkinii on Seed Germination and Seedling Growth of Alfalfa. Acta Agrestia Sinica 30:394 (in Chinese)

Liu G Z, Liu L H, Guo J, Su H Y, Lan Q, Liu G H (2022) The Allelopathic Effect of Aqueous Extracts of *Stellera chamaejasme* on Seed Germination and Seedling Growth of Allium senescens. Acta Agrestia Sinica 30:2391

Liu S B, Yin G M, Alatanqiqige, Qigeqi, Lu P F, Eridunqimuge, Wurina, Meng W J, Galiwa, Wang H L (2022) Establishment of Indexes for Classifying Hazard Grade of *Stellera chamaejasme* L. Animal Husbandry and Feed Science 43:108-113

Liu X, Guan H, Song M, Fu Y, Han X, Lei M, Ren J, Guo B, He W, Wei Y (2018) Reference gene selection for qRT-PCR assays in *Stellera chamaejasme* subjected to abiotic stresses and hormone treatments based on transcriptome datasets. PeerJ 6:e4535

Liu Y J, Meng Z J, Dang X H, Song W J, Zhuo B (2019) Allelopathic effects of *Stellera*

https://doi.org/10.1017/wsc.2025.10056 Published online by Cambridge University Press

chamaejasme on seed germination and seedling growth of alfalfa and two forage grasses. Acta Prataculturae Sinica 28:130-138

Liu Y M, Dong X Z, Li X Y, Zhu Z M, Li Y Y (2024) Spatial pattern of degraded alpine communities invaded by *Stellera chamaejasme* and environmental interpretation in the central Qilian Mountain. Journal of Plant Protection 51:1248-1258 (In Chinese)

Liu Y M, Dong X Z, Long Y Q, Zhu Z M, Wang L, Ge X H, Li J Z (2022) Classification of *Stellera chamaejasme* communities and their relationships with environmental factors in degraded alpine meadow in the central Qilian Mountains,Qinghai Province. Acta Prataculturae Sinica 31:1-11 (in Chinese)

Luo W L, Zhang B, Fang Q E (2021) Advances in population ecology and reproductive biology of *Stellera chamaejasme*. Journal of Zhejiang A 38:193-204

Marzano R, Lingua E, Garbarino M (2012) Post-fire effects and short-term regeneration dynamics following high-severity crown fires in a Mediterranean forest. iForest 5:93–100

O'Dwyer J P, Cornell S J (2018) Cross-scale neutral ecology and the maintenance of biodiversity. Scientific Reports 8:10200

Pan J, Su J C, Liu Y H, Deng B, Hu Z F, Wu J L, Xia R F, Chen C, He Q, Chen J C, Wan L S (2021) Stelleranoids A–M, guaiane-type sesquiterpenoids based on [5,7] bicyclic system from *Stellera chamaejasme* and their cytotoxic activity. Bioorg Chem 115:105251

Ren G H, Deng B, Shang Z H, Hou Y, Long R J (2013) Plant communities and soil variations along a successional gradient in an alpine wetland on the Qinghai-Tibetan Plateau Ecol Eng 61:110-116

Ren H, Zhao C Z, An L J (2015) Spatial point patterns of *Stellera chamaejasme* and *Stipa krylovii* populations in degraded grassland of Noxious and Miscellaneous types based on Ripley's K(r) function. Journal of Arid Land Resources and Environment 29:59-64

Selenge T, Vieira S F, Gendaram O, Reis R L, Tsolmon S, Tsendeekhuu E, Ferreira H, Neves N M (2023) Antioxidant and anti-inflammatory activities of *Stellera chamaejasme* L. roots and aerial parts extracts. Life 13:1654

Song Q, Li S F, Cheng Z Y, Song S J, Huang X X (2023) Chemical constituents from *Stellera chamaejasme* L. and chemotaxonomic significance. Biochem Syst Ecol 107:104602

Stoyan D, Stoyan H (1994) Fractals, Random Shapes, and Point Fields: Methods of Geomet-

rical Statistics. Wiley, Chichester, 408 p

Tang Z H, Yu Q S, Liu H J, Jiang S X, He F L, Zhang Y H, Wang F L, Zhang Y N, Zhao H R, Zhao P (2020) Characteristics of alpine vegetation community and its relationship to topographic climate factors in the eastern Qilian mountain. Acta Ecologica Sinica 40:223-232 (in Chinese)

Wang H, Ma Q C, Geng P S, Feng K, Wu C C, Wang J G, Zhao B Y (2015) Research progress on Daphne mezereum in natural grasslands. Progress in Veterinary Medicine 12:154-160

Wang K, Wang T, Ren C, Dou P, Miao Z, Liu X, Huang D, Wang K (2022) Aqueous extracts of three herbs allelopathically inhibit lettuce germination but promote seedling growth at low concentrations. Plants 11:486

Wang X, Ji M F, Zhang Y H, Zhang L, Akram M A, Dong L W, Deng J M (2023) Plant trait networks reveal adaptation strategies in the drylands of China. BMC Plant Biol 1:266-266

Wiegand T, Moloney K A (2004) Rings, circles, and null-models for point pattern analysis in ecology. Oikos 104:209–229

Wiegand T, Wang X, Anderson-Teixeira K J, Bourg N A, Cao M, Ci X, Davies S J, Hao Z, Howe R W, Kress W J, Lian J, Li J, Lin L, Lin Y, Ma K, McShea W, Mi X, Su S H, Sun I F, Wolf A, Ye W, Huth A (2021) Consequences of spatial patterns for coexistence in species-rich plant communities. Nat Ecol Evol 5:965-973

Wiegand T, Wang X, Fischer SM, Kraft NJ, Bourg NA, Brockelman WY, Cao G, Cao M, Chanthorn W, Chu C, Davies S (2023) Latitudinal scaling of aggregation with abundance and its consequences for coexistence in species rich forests. bioRxiv. 2023 May 21:2023-05. https://doi.org/10.1101/2023.05.03.539324

Wu K, Liu Q, He Y, Chen R (2014) Nutlet morphology and taxonomic significance of Boraginoideae in China. Bulletin of Botanical Research 34:295-308 (in Chinese)

Yan Z Q, Guo H R, Yang J Y, Liu Q, Jin H, Xu R, Cui H Y, Qin B (2014) Phytotoxic flavonoids from roots of *Stellera chamaejasme* L. (Thymelaeaceae). Phytochemistry 106:61–68

Yan Z Q, Zeng L M, Jin H, Qin B (2015) Potential ecological roles of flavonoids from Stellera chamaejasme. Plant Signaling Behav 10:e1001225

You Y F, Ma Q C, Guo Y Z, Kong Y Z, Shi F Y, Wu C C, Zhao B Y (2018) Hazard status and

control countermeasures of poisonous weeds in natural grasslands of Inner Mongolia. Progress in Veterinary Medicine 39:105–110

Zhang N, He J, Xia C, Lian W, Yan Y, Ding K, Zhang Y, Xu J, Zhang W (2021) Ethnopharmacology, phytochemistry, pharmacology, clinical applications and toxicology of the genus Stellera Linn.: A review. J Ethnopharmacol 264:112915

Zhang R, Tielbörger K (2020) Density-dependence tips the change of plant–plant interactions under environmental stress. Nat Commun 11:2532

Zhang W, Gao J M, Zhang A D, Zhang Q L, Wang H X, Sun J (2016) Research progress on secondary metabolites of *Stellera chamaejasme*. Animal Husbandry and Feed Science 37:35–38

Zhang Y H, Volis S, Sun H (2010) Chloroplast phylogeny and phylogeography of *Stellera chamaejasme* on the Qinghai-Tibet Plateau and in adjacent regions. Mol Phylogenet Evol 57:1162–1172

Zhang Y H, Yue J P, Sun H (2015) Identification of twelve novel polymorphic microsatellite loci in the severe weed, *Stellera chamaejasm*e L. (Thymelaeaceae). J Genet 94:24–26

Zhang Y, Cui Z, Wang T, Cao C (2021) Expansion of Native Plant *Stellera chamaejasme* L. Alters the Structure of Soil Diazotrophic Community in a Salinized Meadow Grassland, Northeast China. Agronomy 11:2085

Zhao C Z, Gao F Y, Wang X P, Sheng Y P, Shi F X (2010) Fine-scale spatial patterns of *Stellera chamaejasme* population in degraded alpine grassland in upper reaches of Heihe, China. Chin J Plant Ecol 34:1319–1326

Zhao M D, Wang W Y (2011) Chemical Composition Pharmacognostic Identification and Biological Characteristis of *Stellera chamaejasme* L. J Qinghai Natl Univ 31:60–64 (in Chinese)

Zhu X R, Li X T, Xing F, Chen C, Huang G H, Gao Y (2020) Interaction between root exudates of the poisonous plant *Stellera chamaejasme* L. and arbuscular mycorrhizal fungi on the growth of Leymus chinensis (Trin.) Tzvel. Microorganisms 8:364

https://doi.org/10.1017/wsc.2025.10056 Published online by Cambridge University Press

Table 1. Basic climate details of the sample plot

Location	Altitude m	North latitude	East Longitude	Average annual temperature °C	Average annual precipitation mm
TZ	2964	37°12′45″	102°46′23″	-2	400
HC	2373	37°59′52″	101°38′55″	2	260
XS	2300	38°33′40″	100°17′9″	3.4	300
JM	2768	38°3 ′2 ″	101°17′9″	3	388
KL	2608	38°48′28″	99°53′23″	2	300

https://doi.org/10.1017/wsc.2025.10056 Published online by Cambridge University Press

Table 2. Age grading standards for *S. chamaejasme*.

Ageclass	Growthstage	Number of branches	Height of plant cm	Agees timation years
I	Seedlings (not flowering)	1	3.4 - 8	1 - 2
II	Young plants (occasionally flowering)	1 - 2	13.6 - 24	3 - 6
III	Mature (flowering)	3 - 10	17 - 24	6 -
IV	Mature (flowering)	11 - 20	15 - 20.5	7 - 8
V	Mature (flowering)	21 - 30	17 - 25	8 - 9
VI	Mature (flowering)	31 - 40	17 - 26	9 - 10
VII	Mature (flowering)	41 - 50	15 - 24	10 - 12
VIII	Mature (flowering)	51 - 60	21 - 27	11 - 12
IX	Mature (flowering)	61 - 100	19.5 - 27	12 - 13
X	Mature (flowering)	> 100	20 - 31	12 - 14

https://doi.org/10.1017/wsc.2025.10056 Published online by Cambridge University Press

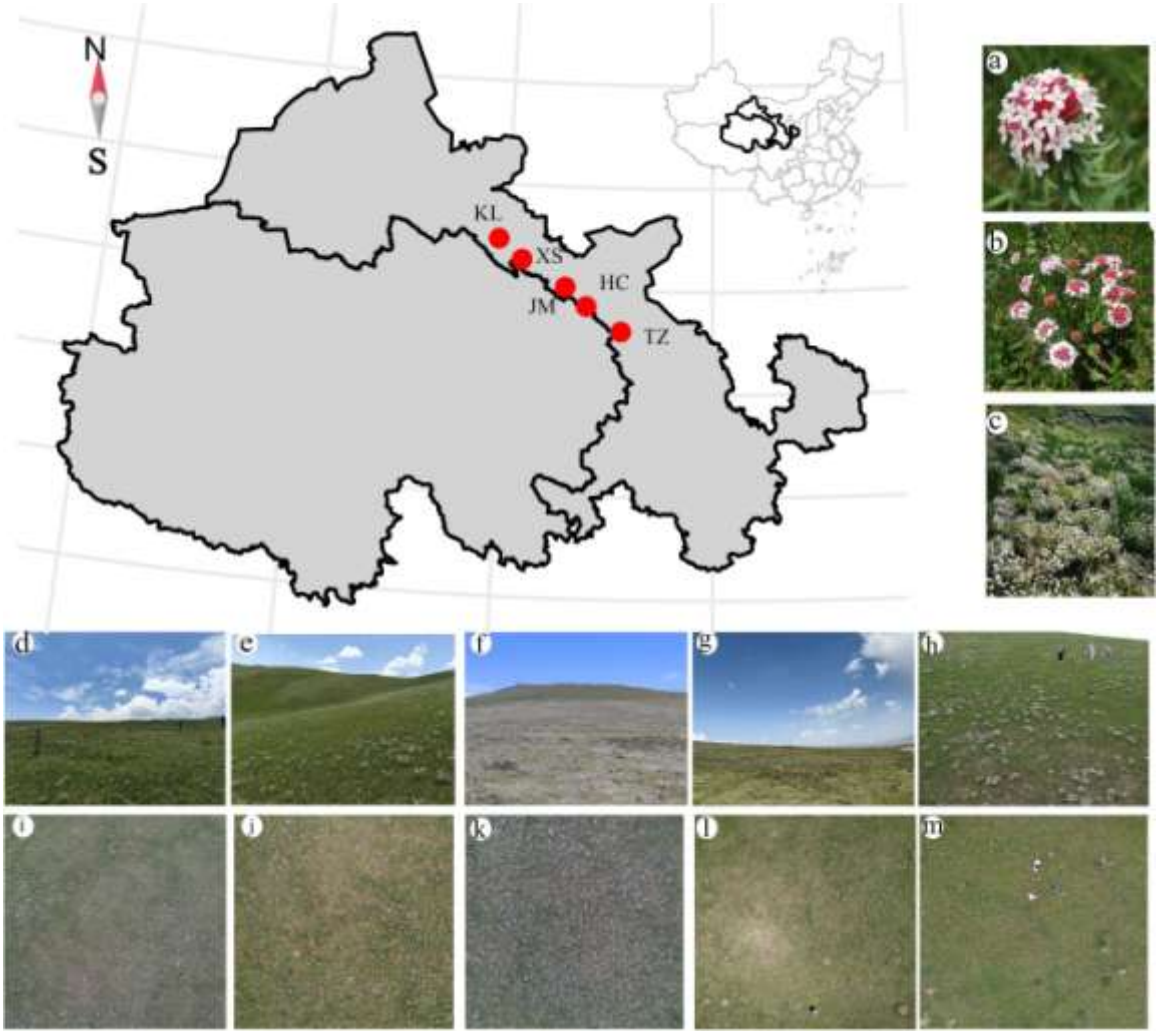

Figure 1. Display of sample plot landscape. panels a, b, and c: *S. chamaejasme* inflorescence (a), individual plant (b), and population (c), respectively. Habitat images (d-h) and corresponding drone images (i-m) are shown for sample sites HC (d, i), JM (e, j), KL (f, k), TZ (g, l), and XS (h, m).

https://doi.org/10.1017/wsc.2025.10056 Published online by Cambridge University Press

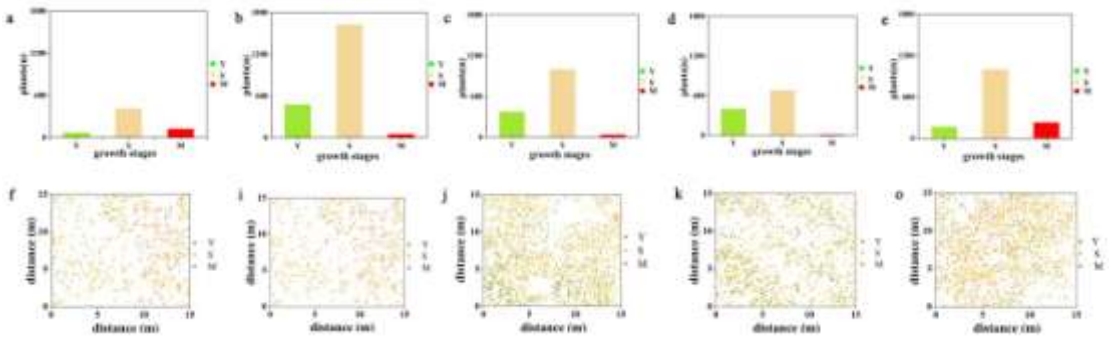

Figure 2. The quantity and spatial distribution of the three age groups of *Stelera chamaejasme*

https://doi.org/10.1017/wsc.2025.10056 Published online by Cambridge University Press

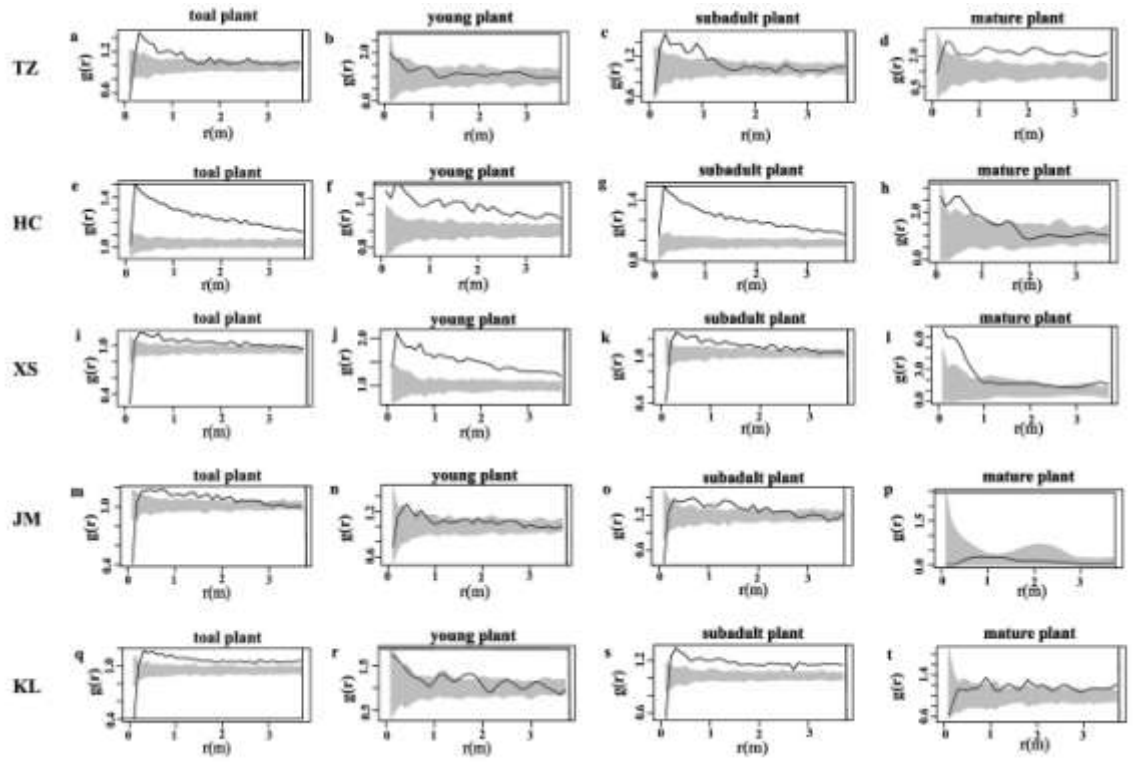

Figure 3. Spatial point patterns of *S. chamaejasme* individuals across five study sites.

each row corresponds to a distinct study site TZ: a-d, HC: e-h, XS: i-l, JM: m-p, KL: q-t. within each site panel, columns (from left to right) depict the spatial distributions of young plants, subadult plants, and mature plants.

https://doi.org/10.1017/wsc.2025.10056 Published online by Cambridge University Press

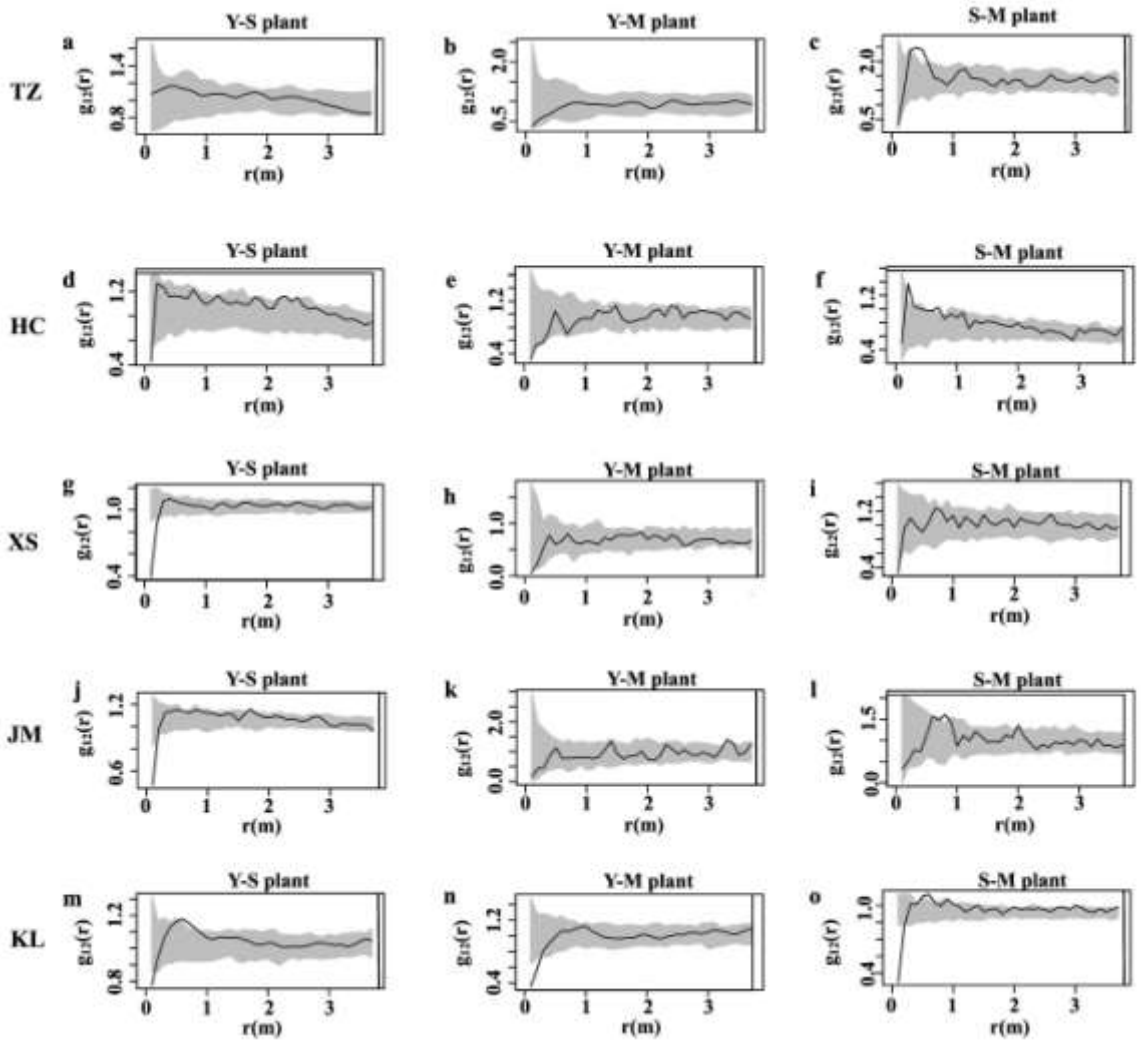

Figure 4. Correlation between different age classes of *S. chamaejasme* in five study sites. each row corresponds to a distinct study site TZ: a-c, HC: d-f, XS: g-i, JM: j-l, KL: m-o. within each site panel, columns (from left to right) depict the spatial associations among different plant cohorts. Young plants and subadult plants (Y-S), young plants and mature plants(Y-M), subadult plants and mature plants(S-M)

https://doi.org/10.1017/wsc.2025.10056 Published online by Cambridge University Press

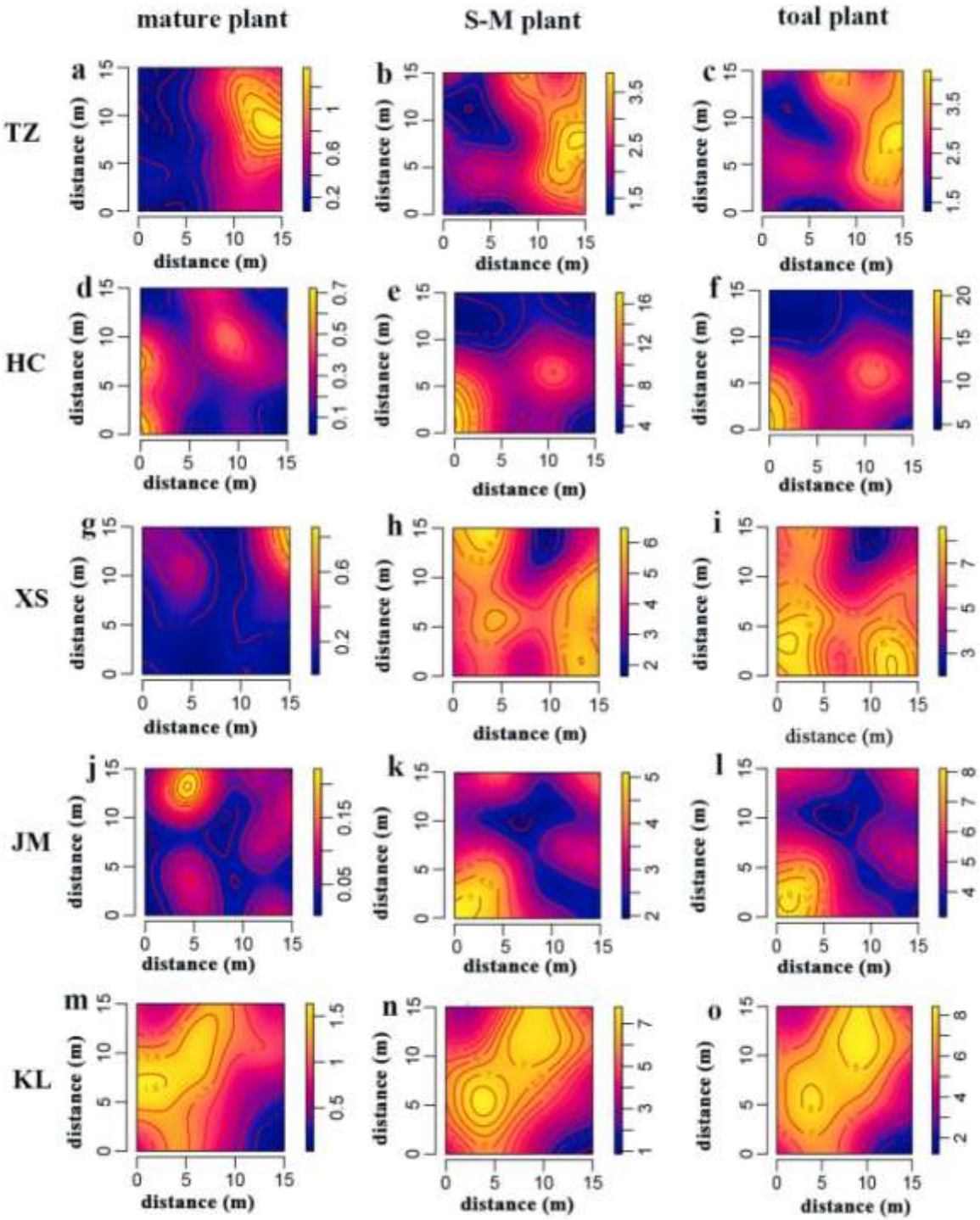

Figure 5. Density of different age classes of *S. chamaejasme* in five study sites.

each row corresponds to a distinct study site TZ: a-c, HC: d-f, XS: g-i, JM: j-l, KL: m-o. each column represents the density distribution for a specific plant group. subadult plants and mature plants(S-M). color bar: kernel density estimate; blue to yellow indicates low to high plant density.

https://doi.org/10.1017/wsc.2025.10056 Published online by Cambridge University Press